University of Bahrain

Journal of the Association of Arab Universities for Basic and Applied Sciences

www.elsevier.com/locate/jaaubas
www.sciencedirect.com

Determination of iron, cobalt and nickel ions from aqueous media using the alkali modified miswak

E.A. Moawed [a],*, M.A. El-ghamry [b], M.A. El-Hagrasy [a], M.F. El-Shahat [c]

[a] Chemistry Department, Faculty of Science, Damietta University, New Damietta, Egypt
[b] Chemistry Department, Faculty of Education, Ain Shams University, Cairo, Egypt
[c] Chemistry Department, Faculty of Science, Ain Shams University, Cairo, Egypt

Abstract   This paper describes a simple, rapid, inexpensive method for the preparation of a new biosorbent based on the modification of miswak fibers by NaOH (AT-Miswak-F). The synthesized AT-Miswak-F sorbent was utilized as an efficient sorbent for the extraction and preconcentration of iron group metal ions from various water samples. In this study, it was found that Fe(III), Co(II) and Ni(II) ions were completely extracted (100%) at pH range of 3–7 and flow rate of 0.3–2.0 mL min^{-1}. Also, the sorption capacity of AT-Miswak-F for Fe(III), Co(II) and Ni(II) are 0.54, 0.24 and 0.15 mmol g^{-1}, respectively. Equilibrium was best described by Freundlich isotherm model ($R^2 = 0.793$) and the initial rate constants were 0.077, 0.054 and 0.035 mmol g^{-1} min^{-1}, respectively. Under the optimized conditions, the method exhibited a detection limit of 1.4, 2.8 and 2.1 ng mL^{-1} for Fe(III), Co(II) and Ni(II) ions in water samples with relative standard deviations of 2.6% ($n = 4$). The method was successfully applied for the determination of Fe(III), Co(II) and Ni(II) ions in sea, ground and contaminated water samples.

1. Introduction

Iron has an essential role in life and a range of biochemical reactions in the living organisms. Iron–proteins are found in all living organisms, ranging from the evolutionarily primitive archaea to humans (Kassem and Amin, 2013; Pourjavid et al., 2014). Cobalt is also beneficial for humans since it is a metallo-cofactor in vitamin B12 (cobalamin); which contributes to the prevention of pernicious anemia and production of red blood cells and has a key role in the normal functioning of the brain and nervous system (Wen et al., 2013; Naushad et al., 2015a). Nickel is used in many industries such as stainless steel, nickel cast irons, alnico magnets, coinage, rechargeable batteries, electric guitar strings, and plating and as a green tint in glass (Gómez-Nieto et al., 2013).

Pollution from chemicals products is a real threat to the aquatic environment, air, and soil (El Haddad et al., 2012). Heavy metals are unpleasantly affecting our ecosystem due to their toxicological and physiological effects in environment (Naushad and AL-Othman, 2015). These metals, if present beyond certain concentration can be a serious health hazard which can lead to many disorders in normal functioning of human beings and animals (AL-Othman et al., 2012). Determi-

---

* Corresponding author at: P.O. Box 34517, Damietta, Egypt. Fax: +20 572403868.
  E-mail address: eamoawed@yahoo.com (E.A. Moawed).

nation of Fe, Co and Ni ions in water samples is to some extent problematic because of the high concentration of interfering matrix components. Preconcentration and separation procedures have been proposed to overcome this problem (Naushad et al., 2014; Awual et al., 2015; Naushad et al., 2015b). Methods employing biosorbents are recommended for the preconcentration and separation studies due to their simplicity and environmentally friendliness (He and Chen, 2014). Moreover, they offer improvements in the sensitivity and selectivity of spectrophotometric methods for the determination of many metal ions (Oguz and Ersoy, 2014). The root of *salvadora persica* tree (miswak) is used as a natural toothbrush (Aboul-Enein, 2014; Naeini et al., 2014) since it contains fluoride salts, detergents, antiseptics, and enzyme inhibitors (Alili et al., 2014). In previous studies, we used the miswak for the extraction of some organic dyes (Moawed and Abulkibash, 2012; Moawed, 2013). Though miswak is an excellent sorbent, the leaching of some of its components hinders its application. This problem necessitates the preparation of a chemically stable miswak for extraction purposes. To improve their properties, biosorbents were modified with different reagents including KOH, $ZnCl_2$ and/or C_6H_{12} (AL-Othman et al., 2012; Alshehri et al., 2014; Nadeem et al., 2014).

This paper describes a simple, rapid, inexpensive procedure with available versatile techniques for the preparation of a new biosorbent by the treatment of miswak fibers with an alkali (NaOH) to eliminate the problem of leached compounds. The AT-Miswak-F was characterized by IR and UV/Vis spectroscopy, SEM and elemental analysis. Parameters controlling the sorption of Fe(III), Co(II), and Ni(II) ions onto AT-Miswak-F, including pH, initial concentrations, shaking time and solution temperature were optimized.

2. Experimental

2.1. Instruments

Iron, cobalt and nickel ions were determined using a Shimadzu UV-1800 spectrophotometer (Shimadzu Corporation, Japan). A glass mini column 10 cm long and 1.0 cm in diameter was used for dynamic procedure. pH measurements were carried out by a Jenway pH meter model 3510, (U.K). Conductivity was performed using a Conductivity Meter (Jenway, model 4071, U.K).

2.2. Reagents and materials

Stock solutions of iron(III), cobalt(II) and nickel(II) (1 mg mL^{-1}) were prepared by dissolving appropriate amounts of iron(III) sulfate, cobalt(II) nitrate and nickel(II) nitrate salts (Fluka) in distilled water containing 1 mL of concentrated HNO_3 (Adwic, Egypt). *Salvadora persica* sticks (Miswak) were obtained from a plantation in El-Khtrichia, El-Qtif, Saudi Arabia.

2.3. General procedures

Alkali-treated miswak fibers (AT-Miswak-F) were prepared by blending miswak sticks (Miswak-F) in a food-processing blender, and then Miswak-F powder was soaked in 1 mol L^{-1} solution of NaOH for 24 h. AT-Miswak-F was filtered off then washed with distilled water, dried at 100 °C and sieved (particle size > 250 μm).

A portion of 0.05 g of the AT-Miswak-F was agitated with 25 mL solution of the tested metal ions for 60 min at 25 °C. The solutions were filtrated and the remaining Fe(III), Co(II) and Ni(II) concentrations was measured spectrophotometrically (Marczenko, 1986).

A 25 mL of the tested metal solutions (1 μg mL^{-1}) were passed through the AT-Miswak-F–containing columns at a flow rate of 1 mL min^{-1}. Metal ions were eluted from the AT-Miswak-F columns by 1 mol L^{-1} HCl. The eluates of metal ions were determined spectrophotometrically.

The tests of addition/recovery of different amounts of iron were performed for the underground water of Dammam city. A 0.1 g portion of the AT-Miswak-F was mixed with 25 mL of water sample which spiked with 20–125 μg of iron(III) then the batch procedure was applied.

To estimate the accuracy of the presented procedure for determination of iron in water; underground water of Nestle SA (Springer Water Factory Co Ltd), sea water of Arabian Gulf in Dammam city have been investigated using batch technique. Collection and determination of iron (III), cobalt (II) and nickel (II) ions in industrial wastewater of from the cooling pond of the casting iron company in Dammam city (spiked with 20 μg of metal ions) using dynamic technique has been investigated.

Density of AT-Miswak-F measurement was carried out in a 25 mL density bottle (pycnometer). The AT-Miswak-F was added to the density bottle with gentle tapping to ensure the settlement of the particles to the bottom; water was then added to the pycnometer in a way to fill all air spaces with water. Chemical composition of AT-Miswak-F, pH$_{ZPC}$, iodine number, density, electrical conductivity, acidic and basic sites were estimated according to procedure described elsewhere (Ververis et al., 2007; Moawed, 2013; Moawed et al., 2014).

3. Results and discussion

3.1. Characteristics of AT-Miswak-F

The densities of Miswak-F and AT-Miswak-F are 0.52 and 0.37 g cm^{-3}, respectively (Table 1). AT-Miswak-F (miswak after treatment by NaOH solution) is less dense than the normal one. This is due to hydrolysis of plant pigments, lipids and mineral salts and these fractions were leached out from the Miswak-F. Also, the hydrolysis process is leading to the increase in spaces, channels, and pores.

Table 1 Chemical and physical properties of miswak fibers and alkali treated miswak fibers.

Property	Miswak-F	AT-Miswak-F
Color	Yellow	Brown
Water solubility (g L^{-1})	3.27	0.56
Electrical conductivity (mS cm^{-1})	1.74	0.19
Bulk density (g cm^{-3})	0.52	0.37
pH$_{ZPC}$	5.20	4.62
Iodine number (mmol/g)	3.10	5.15

The values of electrical conductivity are 1.74 and 0.19 mS/cm for 1% solution of Miswak-F and AT-Miswak-F, respectively (Table 1). This result indicates the chemical stability of the AT-Miswak-F in aqueous solution when compared with that of the Miswak-F.

IR spectra of Miswak-F in KBr pellets were collected. Table 2 shows the IR main spectral bands of Miswak-F and AT-Miswak-F recorded in the spectral range of 400 and 4000 cm^{-1}. From the obtained results, it is clear that the spectral bands of AT-Miswak-F are shifted to higher frequency compared to those of the Miswak-F. This result may be attributed to the leaching out of some mineral salts in addition to the hydrolysis of some of the miswak matrix into free functional groups.

C, H, N, S and O percentages of Miswak-F and AT-Miswak-F were estimated. The results show that carbon and hydrogen percentages of the AT-Miswak-F (45.1 and 5.8%) are greater than those of the Miswak-F (34.5 and 4.5%). However, the percentages of nitrogen, sulfur and oxygen decreased due to the leaching out of some mineral salts. The obtained results show that the AT-Miswak-F consists mainly of hydrocarbon compounds *e.g.* lignin and cellulose.

The Surface morphology of Miswak-F and AT-Miswak-F was investigated using scanning electron microscopy (SEM) at magnifications from 100 to 3000×. The images of Miswak-F and AT-Miswak-F (400–800×) are shown in Fig. 1. The microstructure of the miswak fibers reveals that spaces, channels and pores of miswak fibers increased after alkali treatment. Also, the surface of AT-Miswak-F contains many pores with pore size between 50 μm and 500 μm (Fig. 2), indicating its suitability for metal ions sorption.

The electronic spectra of Miswak-F and AT-Miswak-F were recorded using Nujol mulls method. The UV spectrum of Miswak-F shows many peaks between 200 and 400 nm (381, 219, 212 and 205 nm, Table 2) attributed to its numerous functional groups. These peaks are slightly shifted (360, 217, 208 and 202 nm) in the AT-Miswak-F spectra (blue shift, Table 2). This may be due to the hydrolysis of the functional groups of the Miswak-F.

The values of pH$_{ZPC}$ of both the Miswak-F and AT-Miswak-F are 5.2 and 4.6, respectively, indicating their acidic character (Fig. 3a). The surface of the AT-Miswak-F is positively charged at pH < 4.6; however, the surface sites are negatively charged at pH > 4.6. The positive charge of the surface of the AT-Miswak-F in acidic medium is due to the protonation of oxygen atoms of cellulose and lignin. The negative
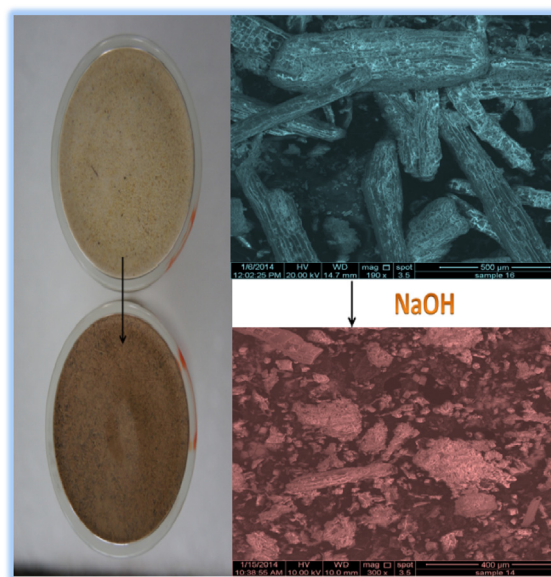

Figure 1 The SEM images of Miswak-F and AT-Miswak-F at magnifications of 400 and 800×.

charge of the surface of the AT-Miswak-F would be attributed to the deprotonation of the phenolic and carboxylic groups. The pH$_{ZPC}$ value of the AT-Miswak-F is lower than that of the Miswak-F. This may be attributed to the decrease in the basic functional groups after the treatment with NaOH solution. Due to the buffering effect of water on Miswak-F and AT-Miswak-F surfaces; the pH measurements are only considered in the pH ranges of 4–10.8 and 4.8–7.5, respectively (Fig. 3b).

The iodine number gives information about the internal surface of an adsorbent; since it is assumed to measure the surface area in micropores within pore sizes ⩾10 Å (Daifullah et al., 2003). The iodine molecule has an area of 0.15–0.42 nm^2, therefore it can fit into the micropores of sorbent particles, providing information about the internal surface (Attia et al., 2006). The iodine number of both Miswak-F and AT-Miswak-F are 3.1 (396.9 mg g^{-1}) and 5.2 mmol g^{-1} (653.8 mg g^{-1}), respectively (Table 1). Based on the value of the iodine number, the AT-Miswak-F exhibits better surface area when compared to activated carbon synthesized from jatropha husk (70 mg g^{-1}) (Namasivayam et al., 2007), rice husk (122 mg g^{-1}) (Daifullah et al., 2003), eucalyptus sawdust (179 mg g^{-1}) (Martins et al., 2007), coir pith (203 mg g^{-1}) (Namasivayam and Sangeetha, 2005), and rubber wood (300 mg g^{-1}) (Kumar et al., 2006).

Table 3 shows the chemical analyses of Miswak-F and AT-Miswak-F. Miswak-F contains cellulose and hemicellulose 59.5%, lignin 31.6% and ash 8.9%. After alkali treatment, the cellulose/hemicellulose and ash percentages decreased to 41.9% and 1.4%, respectively, while the lignin content increased to 56.7% in the AT-Miswak-F. This shows that lignin is the main component of the AT-Miswak-F. It is worth noting that the AT-Miswak-F has a low ash content (2% or less), which makes it suitable to be a good stable biosorbent.

The total acidic sites estimated for Miswak-F and AT-Miswak-F are 1.4 and 3.5 mmol g^{-1}, respectively (Table 3). The increase in the acidic sites of the AT-Miswak-F is due to

Table 2 Spectra data of miswak fibers and alkali treated miswak fibers.

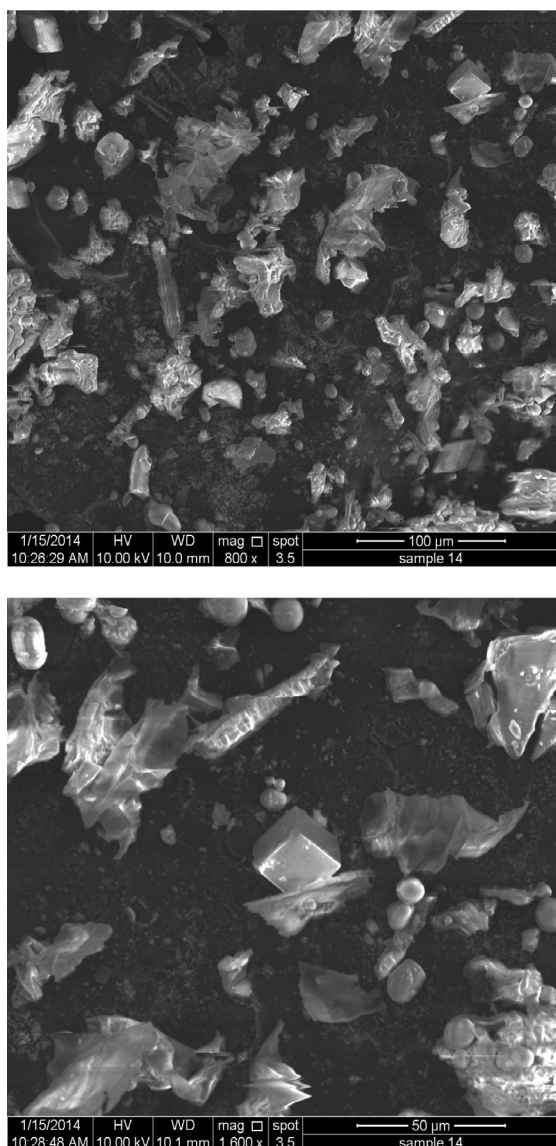| Property	Miswak-F	AT-Miswak-F
IR spectra		
Main strong stretches absorption band (cm^{-1})	3372.9, 2914.9, 1699.9, 1632.5, 1524.7, 1425.2, 1330.3 and 1031.1	3387.35, 2931.06, 1717.3, 1636.3, 1526.53, 1441.53, 1333.54 and 1105.01
UV– spectra		
λ$_{max}$ (nm)	381, 219, 212, 205	360, 217, 208, 202
Elemental analysis		
C, H, N and S%	34.5, 4.5, 2.2 and 3.8	45.1, 5.8, 0.9 and 1.2

Figure 2 Surface morphology of AT-Miswak-F using scanning electron microscopy (SEM) at magnifications 800 and 1600×.

the hydrolysis of the Miswak-F matrix to free functional groups. AT-Miswak-F contains $0.75 \, mmol \, g^{-1}$ of lactonic groups, $0.87 \, mmol \, g^{-1}$ of carboxylic groups, $1.88 \, mmol \, g^{-1}$ of phenolic groups. Also, the total basicity was determined to be $0.5 \, mmol \, g^{-1}$ and as noticed, the acidic sites are greater than the basic sites ($3.5 \, mmol \, g^{-1} : 0.5 \, mmol \, g^{-1} \approx 7:1$).

3.2. Optimum conditions for the extraction of metal ions using miswak fibers

The percentage of the extraction of Fe(III), Co(II) and Ni(II) ions was plotted against the pH value (Fig. 4). The results show that the extraction of Fe(III) and Ni(II) rapidly increased by increasing the pH from 1 to 7 then decreased at pH 9. The maximum extraction efficiency reached 100% for Fe(III) and 78.4% for Ni(II) ions at pH 7, while, the maximum extraction of cobalt (100% Co) was at pH 3. Fe^{3+} and Ni^{2+} are sorbed due to the electrostatic interaction between metal ions (cation)
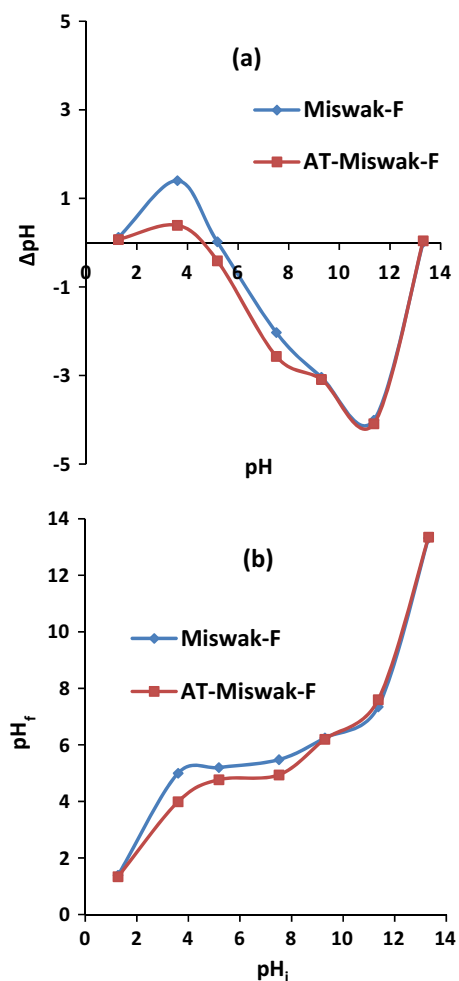

Figure 3 (a) pH_{ZPC} of miswak fiber (Miswak-F) and miswak fibers after alkali treatment (AT-Miswak-F) & (b) effect of initial pH on the Miswak-F and AT-Miswak-F.

Table 3 Composition of miswak fibers and alkali treated miswak fibers.

Property	Miswak-F	AT-Miswak-F
Ash (%)	8.9	1.4
Lignin (%)	31.6	56.7
Cellulose and hemicellulose (%)	59.5	41.9
Total acidity (mmol g^{-1})	1.38	3.50
Phenolic (mmol g^{-1})	0.69	1.88
Carboxylic acid (mmol g^{-1})	0.34	0.87
Lactones (mmol g^{-1})	0.35	0.75
Total basisty (mmol g^{-1})	0.20	0.50

and the negatively charged surface of the AT-Miswak-F. Based on the behavior of Co(II) ions extraction onto the AT-Miswak-F, it can be speculated that chelation may be the principal mechanism, since chelation process requires a proper acidity. The selectivity sequence at the pH range of 1–3 is in the order Co(II) > Fe(III) > Ni(II), while the order is Fe(III) > Co(II) > Ni(II) at pH 7. The separation factors (α) of Co(II)/Fe(III) and Co(II)/Ni(II) are 3.8 and 4.0, respectively at pH 1. The results show that controlling the pH of the
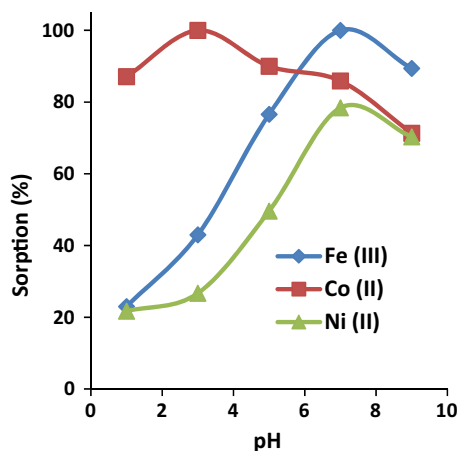
Figure 4 Effect of initial pH on the sorption of iron (III), cobalt (II) and nickel (II) onto AT-Miswak-F.

solution enhances the selectivity of AT-Miswak-F toward the investigated metal ions.

Fig. 5 shows the plot of the amount of sorbed metal per unit mass of AT-Miswak-F versus the initial concentrations of Fe(III), Co(II) and Ni(II) ions. The results show that the plots are linear (average value of intercept 0.003) with good correlation (average value of $R^2 = 0.995$). The capacity values of miswak fibers for iron(III), cobalt(II) and nickel(II) ions were estimated to be 0.54, 0.24 and 0.15 mmol g^{-1}, respectively. The sequence of capacity of miswak fibers for these metal ions is in the order, $Fe^{3+} > Co^{2+} > Ni^{2+}$, which may be ascribed to their different ionic sizes and the reaction between AT-Miswak-F functional groups and metal ions. Also, the AT-Miswak-F exhibits better capacity toward Fe (III) (30.2 mg g^{-1}), Co(II) (14.1 mg g^{-1}) and Ni(II) (8.8 mg g^{-1}) in comparison to other sorbents e.g. SiO$_2$/Nb$_2$O$_5$/ZnO mixed oxide by sol–gel: 0.5 mg Co g^{-1} (Diniz et al., 2014), activated carbon: 11.1 mg Co g^{-1} and 7.8 mg Ni g^{-1} (Dobrowolski and Otto, 2012), Nile blue–grafted polyurethane foam: 15.0 mg Fe g^{-1} (El-Shahat et al., 2003), polyhydroxyl polyurethane foam: 0.5 mg Fe g^{-1}
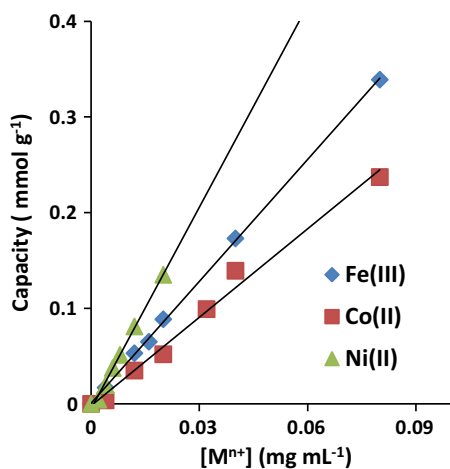

Figure 5 Effect of initial platinum concentration on the extraction of iron (III), cobalt (II) and nickel (II) onto AT-Miswak-F.

(Moawed et al., 2013), chromosorb 108: 4.7 Co mg g^{-1} and 4.9 mg Ni g^{-1} (Tuzen et al., 2005), chitosan polymers: 3.4 mg Co g^{-1} and 3.1 mg Ni g^{-1} (Emara et al., 2011), zeolite: 2.0 mg Ni g^{-1} (Alvarez-Ayuso et al., 2003) and vermiculite: 0.2 mg Ni g^{-1} (Blais et al., 2003).

Limits of detection (LOD = 3 σ) and quantification (LOQ = 10 σ) for iron(III), cobalt(II) and nickel(II) ions were calculated. The values of LOD of Fe(III), Co(II) and Ni(III) are 1.4, 2.4 and 2.1 ng mL^{-1}, respectively, while the LOQ values of Fe(III), Co(II) and Ni(II) are 4.7, 8.0 and 7.1 ng mL^{-1}, respectively. The miswak fiber method is more efficient when compared to other methods such as Fe: 2–18 ng mL^{-1} (Merli et al., 2012; Du et al., 2013; Kassem and Amin, 2013), Co: 2.4–6 ng mL^{-1} (Rezaei et al., 2001; Amin, 2014; Zeng et al., 2012; Xu et al., 2013) and Ni: 1.7–13 ng mL^{-1} (de Sousa and Korn, 2001; Rezaei et al., 2001; Amin and AL-Attas, 2012; Xu et al., 2013). The average recovery percentage values are 98.4% Fe(III), 100% Co(II) and 76.0% Ni(II) with low relative standard deviation values (RSD = 2.0, 2.3 and 3.7%, respectively, $n = 4$), which indicates both good precision and accuracy of the proposed method for the determination of iron, cobalt and nickel.

The effect of temperature (25–90 °C) on the extraction of iron, cobalt and nickel onto miswak fibers was studied. The maximum extraction of Fe(III) and Co(II) ions (99–100%) was observed at low temperature, while the sorption of Ni (II) ions increased by increasing the temperature. The sorption capacities of AT-Miswak-F for Fe(III) and Co(II) decreased by increasing the temperature, while the capacity for Ni(II) increased. This shows that this method is more efficient for the sorption of nickel disposed from hot wastewater–industries. Also, this reveals that the chemisorption of both iron (III) and cobalt(II) is exothermic while it is endothermic for nickel(II).

The effect of flow rate of Fe(III), Co(II) and Ni(II) solutions (0.3–4.0 mL min^{-1}) through the miswak fibers column was studied. The maximum recovery was observed in the range 0.3–2.0 mL min^{-1} and the recovery percentage decreased from 100% to 97.8% with increasing flow rate from 2 to 3.5 mL min^{-1}.

The effect of various eluting agents on the stripping of iron from miswak column was tested. It was observed that Fe(III), Co(II) and Ni(II) ions were completely eluted by HCl solution. The effect of different concentrations of HCl (0.05–1.0 mol L^{-1}) on the desorption of the retained iron(III), cobalt(II) and nickel(II) ions on the miswak fibers–columns was studied. A concentration of 0.5 mol L^{-1} (25 mL) was found to be the minimum concentration of HCl necessary for the complete elution of Fe(III), Co(II) and Ni(II).

The effect of foreign ions (200 µg) on the determination of iron, cobalt and nickel ions (5 µg) was studied. Al^{3+}, Cr^{3+}, Fe^{2+}, Cd^{2+}, Mo^{6+} and Ag^+ ions were found to reduce the sorption of iron ions from 8.6% to 23.4%, while Cu^{2+} and Bi^{3+} caused the greatest interference 59.2 and 51.3%, respectively (Fig. 6). Al^{3+}, Cr^{3+}, Ag^+, Bi^{3+} and Cd^{2+} ions slightly interfered (3.8–18.2%) in the determination of Co^{2+}, while Cu^{2+} and Fe^{2+} ions strongly interfered, 47.9 and 75.6%, respectively. Al^{3+}, Mo^{6+}, Cd^{2+}, Fe^{2+}, Cr^{3+}, Bi^{3+} and Ag^+ ions have a slight interference (2.9–18.3%) in the determination of Ni^{2+}, while Cu^{2+} has the strongest interference 92.7%. The addition of phosphate and citrate anions alongside
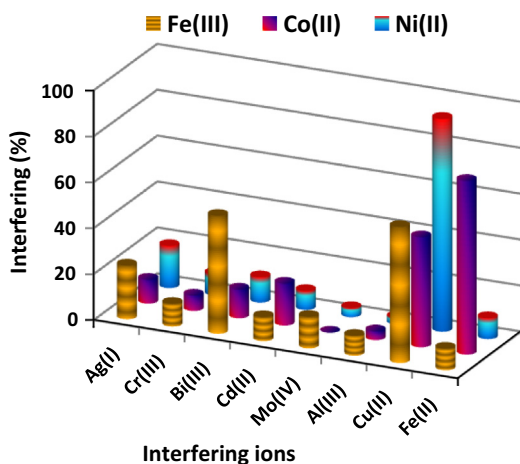
Figure 6 Effect of interfering metal ions on the sorption of iron (III), cobalt (II) and nickel (II) onto AT-Miswak-F.

with adjusting the pH of the solution minimizes the interfering effect.

3.3. Sorption mechanism

The electronic spectral data of the metal: miswak complexes are listed in Table 4. In the region between 200 and 800 nm, the absorption bands of the free AT-Miswak-F fibers appeared at 202, 208, 217 and 360 nm. The higher energy bands at 202, 208, 217 nm are assigned to the intraligand transitions (π–π^*) that are localized on the conjugated system and are largely unaffected by complexation (Shebl et al., 2014). The lower energy band at 360 nm are assigned to n–π^* transition of the carbonyl (C=O) chromophores that overlapped with the charge-transfer (CT) transitions within the molecule. The UV–Vis spectra of the Fe(III), Co(II) and Ni(II) complexes also exhibited similar transition bands but were shifted to lower wavelengths for all of the metal complexes. The results showed that the spectral bands of miswak functional groups are blue shifted, which may be due to the chelation with the metal ions. The electronic spectra of metal: miswak complexes exhibited new bands at 373 and 384 nm for iron(III) miswak complex, 364 and 394 nm for cobalt(II) miswak complex and 375 and 390 nm for nickel(II) miswak complex. These new bands may be assigned to the intermolecular ligand–metal charge transfer transition LMCT (El-ghamry et al., 2013).

The electronic spectra of metal miswak complexes showed two bands in the visible region at 444 and 643 nm for iron (III) miswak complex, 422 and 646 nm for cobalt(II) miswak complex and 448 and 647 nm for nickel(II) miswak complex. For iron(III) miswak complex, the first band at 444 nm is assigned to a charge transfer band (MLCT) and the second band at 643 nm is a d–d transition which can be assigned to $^6A_1 \rightarrow {}^4T_2$ electronic transition and provides an evidence for octahedral arrangement around the iron(III) ion (Ismail et al., 2012). For cobalt (II) miswak complex, the two bands at 422 and 646 nm can be assigned to $^4T_{1g}(F) \rightarrow {}^4T_{1g}(P)$ and $^4T_{1g}(F) \rightarrow {}^4A_{2g}(F)$ transitions, respectively, and indicates that the geometry around cobalt(II) ion is octahedral (Emara et al., 2011). For nickel (II) miswak complex, the two bands at 448 and 647 nm can be assigned to $^3A_{2g}(F) \rightarrow {}^3T_{1g}(P)$ and $^3A_{2g}(F) \rightarrow {}^3T_{1g}(F)$ transitions, respectively, suggesting an octahedral geometry around nickel(II) ion.

The conductivities of the metal miswak complexes in aqueous solutions (1%) were measured at room temperature and the results are listed in Table 4. The observed conductivity values for iron (III), cobalt (II) and nickel (II) miswak complexes are 0.34, 0.24 and 0.15 mS/cm respectively, suggesting the non-electrolytic nature of all complexes. The neutrality of these complexes may be attributed to either partial de-protonation of the phenolic (OH) or carboxylic (O=C–OH) groups of the free AT-Miswak-F during the complexation with the metal ions, and/or coordination with the anions (SO_4^{2-} or NO_3^- ions) of the metal salts.

The percentages of carbon, hydrogen, nitrogen, sulfur and oxygen elements of the free AT-Miswak-F (45.1%, 5.8%, 0.9%, 1.2% and 47.0%, respectively) changed after complexation with iron(III) (40.5%, 5.5%, 1.2%, 3.0% and 49.8%, respectively), cobalt(II), (41.7%, 5.7%, 4.5%, 0.6%, 47.5%, respectively) and for nickel(II) (44.5%, 6.0%, 5.9%, 0.4% and 43.2%, respectively). The decrease in the carbon and hydrogen contents of the corresponding AT-Miswak-F–metal complexes indicates the bonding between AT-Miswak-F fibers and the metal ions (Fe^{3+}, Co^{2+} and Ni^{2+}) and provides an evidence for complex formation. The decrease in the carbon and hydrogen contents of AT-Miswak-F fibers after complexation with the metal ions is arranged as follows: iron(III) miswak complex > cobalt(II) miswak complex > nickel(II) miswak complex which agrees with the sorption capacity results of miswak fibers: 0.34, 0.24 and 0.15 mmol g^{-1} for the sorption of Fe(III), Co(II) and Ni(II) ions, respectively. The increase in the sulfur and oxygen contents of the iron (III) AT-Miswak-F complex (3.0 and 49.8%, respectively) compared with those of the free AT-Miswak-F (1.2 and

Table 4 Conductivity and electronic spectral data and their assignments for Miswak-F, AT-Miswak-F and metal: AT-Miswak-F complexes.

Material	Electronic spectra (λ_{max}/nm)					Conductivity (mS/cm)
	π–π^* transition	n-π^* overlapped with CT transition	LMCT transition	MLCT transition	d–d transitions	
Miswak-F	205, 212, 219	381	–	–	–	1.74
AT-Miswak-F	202, 208, 217	360	–	–	–	0.19
Iron(III): miswak	201, 205, 207, 213	348, 359	373, 384	444	643	0.34
Cobalt(II): miswak	201, 205, 207, 213	342, 350	364, 394	–	422, 646	0.24
Nickel(II): miswak	201, 205, 207, 213	348, 354	375, 390	–	448, 647	0.15

47.0%, respectively) may be due to the coordination of sulfate groups with iron(III) ions. Also, the increase in the nitrogen content of cobalt(II) (5.9%) and nickel(II) (4.5%) AT-Miswak-F complexes when compared with that of the free AT-Miswak-F (0.9 %) may be attributed to the coordination of the nitrate groups with cobalt(II) and nickel(II) ions. This supports the postulation of the complex formation between AT-Miswak-F and the metal ions (Fe^{3+}, Co^{2+} and Ni^{2+}), as indicated by low conductivity values of the AT-Miswak-F-metal complexes (0.15–0.34 mS/cm).

The stretching vibrations of carbonyl $\upsilon_{(C=O)}$ and phenolic $\upsilon_{(OH)}$, $\upsilon_{(C-O)}$ groups of the AT-Miswak-F-metal complexes were noticed to be shifted when compared to those of the free AT-Miswak-F (Fig. 7). The $\upsilon_{(OH)}$ of the AT-Miswak-F at 3387.35 cm^{-1} was shifted to lower frequencies in the metal miswak complexes (3383.5, 3349.89 and 3358.43 cm^{-1}). This indicates chelation of the phenolic ─OH group to the metal ions via oxygen atoms. The $\upsilon_{(C=O)}$ of the metal miswak complexes was shifted to lower wavenumber (1710.55, 1708.62 and 1712.48 cm^{-1}) compared to that of the AT-Miswak-F at 1717.30 cm^{-1}, indicating the coordination of the C═O groups of the AT-Miswak-F with the investigated metal ions. The $\upsilon_{(C-O)}$ of the phenolic groups of the AT-Miswak-F at 1333.54 and 1105.01 cm^{-1} were shifted to lower frequencies after metal sorption (1328.71 and 1101.16, 1324.86 and 1096.33, 1326.79 and 1103.08 cm^{-1}) suggesting its participation in the chelation. The appearance of extra bands at 435.83, 434.87 and 438.73 for Fe(III), Co(II) and Ni(II) complexes, respectively, could be assigned to the stretching frequencies of the $\upsilon_{(M-O)}$ bands.

From the results of the electronic and IR spectra of the AT-Miswak-F before and after metal sorption, we suggest that the sorption of iron (III), cobalt (II) and nickel (II) ions on AT-Miswak-F occurs principally according to chelation mechanism via the coordination of phenolic (─OH) and carboxylic (O═C─OH) groups with the metal ions.

The data of isotherm curves were analyzed using Langmuir $[C_e/Q_c = (1/K_L b) + (C_e/K_L)]$ and Freundlich $(\log Q_c = \log K_f + \frac{1}{n} \log C_e)$ models, where C_e is the amount of metal sorbed at equilibrium, and K_F, n, K_L and b are constan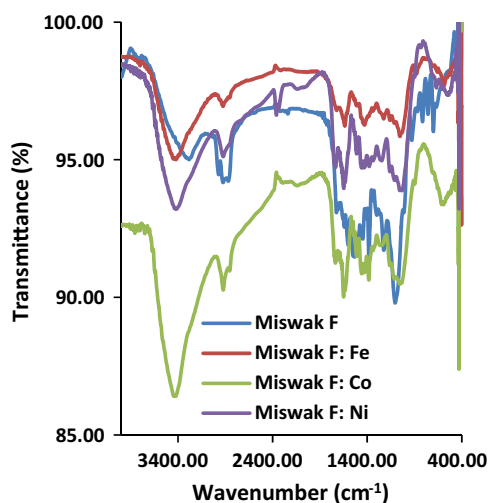ts. The results show that the correlation coefficient values for the sorption of Fe (III), Co (II) and Ni (II) are 0.683, 0.872 and 0.825, respectively. The plot of Q_c/C_e versus C_e for the data according to Langmuir model gives bad linear relationship (R^2 = 0.097, 0.206 and 0.142, respectively) for the sorption of iron, cobalt and nickel onto AT-Miswak-F. This leads to conclude that the surface of the AT-Miswak-F has a heterogeneous structure and the value of $n > 1$ shows the favorable nature of adsorption (Naushad and AL-Othman, 2015).

The diffusion mechanism of the sorption of Fe(III), Co(II) and Ni(II) onto AT-Miswak-F was investigated using Morris-Weber $[Q_t = K_i \sqrt{t}]$ and Reichenberg $[Bt = -0.4977 - \ln (1 - F)]$ & $[F = (6/R)(D_i t/\pi)^{1/2}]$ equations, where Q_e and Q_t are the amount of metal ion sorbed at equilibrium and time t, respectively. k_i is the intraparticle diffusion rate constant (mmol g^{-1} $min^{-1/2}$). The Bt value is a mathematical function of $F = Q_t/Q_e$. D_i is the effective diffusion coefficient. The obtained data show that the plots of Q versus $\sqrt{t}$ are linear and the values of correlation coefficients are 0.996, 0.931 and 0.77, respectively. The diffusion rate constant values of sorption of Fe(III), Co(II), Ni(II) are 8.7, 6.1 and 0.7 μmol g^{-1}-$min^{-1/2}$, respectively. According to the forgoing results, the diffusion rate is rapid. The sequence of diffusion rate was in the order, Fe(III) > Co(II) > Ni(II) which is attributed to their different ionic sizes and nature of the reaction of AT-Miswak-F functional groups with these metal ions. The relation between Bt and t for the sorption of Fe(III), Co(II) and Ni(II) was investigated (average value of R^2 = 0.845). This reflects the formation of partial film along with the intraparticle diffusion. The linear plots of F versus $t^{1/2}$ give the numerical values of effective diffusion coefficient (D_i) from the slope. The values of D_i of the Fe(III), Co(II) and Ni(II) sorption are 9.6×10^{-8}, 9.3×10^{-8} and 0.09×10^{-8} cm^2 min^{-1}, respectively. The film diffusion rate depends on the size of metal ions.

3.4. Analytical applications

Results given in Table 5 show that the removal of iron ions (>95%) from water samples by At-Miswak-F were quantitative. There is a good agreement between added and recovered tested metal ions using batch procedure. The average value of standard deviation for the spiked samples is 2.25%.

The obtained results are given in Table 6. There is a good agreement between the certified analyses and the direct spectrophotometric determination of iron content with batch procedure. This result shows that iron can be determined effectively in sea water and underground water using AT-Miswak-F method. The relative standard deviation values for the water samples are in the average of 1.15% (n = 3). The obtained data conferred susceptible accuracy of the devel-

Figure 7 Infrared spectra of AT-Miswak-F: Metal complexes.

Table 5 Recovery of iron (III) from underground water using AT-Miswak fibers.

Added, μg	Found		
	μg	%	RSD%
20	20.19	100.95	2.25
50	49.53	99.06	
75	74.06	98.75	
125	119.49	95.59	

Table 6 Determination of iron in certified water samples using batch technique.

Sample	Certified analysis $\mu g\,mL^{-1}$	Direct method $\mu g\,mL^{-1}$	Miswak method $\mu g\,mL^{-1}$	RSD %
Arabian Gulf sea water	0.30	0.35	0.32	0.98
Nestle SA underground water	< 0.02	0.19	0.18	1.31

Table 7 Determination of metal ions in wastewater samples using dynamic technique.

Metal ions	Add µg	Found Mg	Recovery %	RSD%
Fe(III)	0	1.64	100	1.69
	20	20.66	103.3	
Co(II)	0	0.40	100	0.00
	20	20	100	
Ni(II)	0	1.22	100	0.28
	20	18.8	94.1	

oped method based on the satisfactory values of RSD% in addition to the reasonably high sensitivity and validity of the proposed method for the determination of iron in different water samples.

The average removal and recovery percentages of metal ions from the wastewater samples are 94–103% (Table 7). The average RSD% values are found to be in the range 0.0–1.7%, which is considered relevant for real samples. The results indicate the suitability of the AT-Miswak-F column for water analysis and the removal of the metal ions from industrial wastewater.

4. Conclusion

It is of great interest to employ agricultural by-products such as Miswak as an economical method for the treatment of wastewater containing metal ions. Our results demonstrate that miswak is an effective adsorbent for the removal of Fe (III), Co(II) and Ni(II) from aqueous solutions with high sensitivity and selectivity. The treatment of miswak fibers by NaOH solution led to the widening of the pore spaces resulting in the increase in the internal surface area of the miswak fibers. The modified sorbent has better capacity toward Fe $(30.2\ mg\,g^{-1})$, Co $(14.1\ mg\,g^{-1})$ and Ni $(8.8\ mg\,g^{-1})$ than other sorbents. The maximum extraction of Fe(III) and Ni (II) ions was at pH 7, while the maximum extraction of cobalt was at pH 3. Kinetics and isotherm studies have confirmed the fast and intensive sorption of the tested metal ions onto miswak fibers. The faster adsorption kinetic data may be useful for environmental technologies in designing heavy metal removal from wastewater plants. The developed procedure is simple, rapid, inexpensive, with high tolerance to interfering ions. The sorption of iron(III), cobalt(II) and nickel(II) ions on miswak fibers occurs principally according to chelation

mechanism, ion association and/or anion exchange. The applicability of the AT-miswak-F was evaluated by the analysis of several real samples. The results indicate that iron group can be determined effectively in seawater and underground water using miswak fiber method. Also, the sorbent is suitable for the removal of metal ions from industrial wastewater. Analytical features such as detection limit, enrichment factor and precision are satisfactory for trace analysis of iron, cobalt and nickel.

References

Aboul-Enein, B.H., 2014. The miswak (*Salvadora persica* L.) chewing stick: cultural implications in oral health promotion. Saudi J. Dent. Res. 5, 9–13.

Alili, N., Türp, J.C., Kulik, E.M., Waltimo, T., 2014. Volatile compounds of *Salvadora persica* inhibit the growth of oral Candida species. Arch. Oral Biol. 59, 441–447.

AL-Othman, Z.A., Ali, R., Naushad, Mu, 2012. Hexavalent chromium removal from aqueous medium by activated carbon prepared from peanut shell: adsorption kinetics, equilibrium and thermodynamic studies. Chem. Eng. J. 184, 238–247.

Alshehri, S.M., Naushad, Mu., Ahamad, T., AL-Othman, Z.A., Aldalbahi, A., 2014. Synthesis, characterization of curcumin based ecofriendly antimicrobial bio-adsorbent for the removal of phenol from aqueous medium. Chem. Eng. J. 254, 181–189.

Alvarez-Ayuso, E., Garcia-Sanchez, Querol X., 2003. Purification of metal electroplating waste waters using zeolites. Water Res. 37, 4855–4862.

Amin, A.S., 2014. Study on the solid phase extraction and spectrophotometric determination of cobalt with 5-(2-benzothiazoly-lazo)-8-hydroxyquinolene. Arabian J. Chem. 7, 715–721.

Amin, A.S., AL-Attas, A.S., 2012. Study of the solid phase extraction and spectrophotometric determination of nickel using 5-(4′-chlorophenylazo)-6-hydroxypyrimidine-2,4-dione in environmental samples. J. Saudi Chem. Soc. 16, 451–459.

Attia, A.A., Rashwan, W.E., Khedr, S.A., 2006. Capacity of activated carbon in the removal of acid dyes subsequent to its thermal treatment. Dyes Pigm. 69, 128–136.

Awual, Md.R., Eldesoky, G.E., Yaita, T., Naushad, Mu., Shiwaku, H., AL-Othman, Z.A., Suzuki, S., 2015. Schiff based ligand containing nano-composite adsorbent for optical copper(II) ions removal from aqueous solutions. Chem. Eng. J. 279, 639–647.

Blais, J.F., Shen, S., Meunier, N., Tyagi, R.D., 2003. Comparison of natural adsorbents for metal removal from acidic effluent. Environ. Technol. 24, 205–215.

Daifullah, A.A.M., Girgis, B.S., Gad, H.M.H., 2003. Utilization of agro residues (rice husk) in small waste water treatment plans. Mater. Lett. 57, 1723–1731.

de Sousa, C.S., Korn, M., 2001. Effects of ultrasonic irradiation on the spectrophotometric determination of nickel with dimethylglyoxime. Anal. Chim. Acta 444, 309–315.

Diniz, K.M., Gorla, F.A., Ribeiro, E.S., do Nascimento, M.B.O., Corrêa, R.J., Tarley, C.R.T., Segatelli, M.G., 2014. Preparation of SiO₂/Nb₂O5/ZnO mixed oxide by sol–gel method and its application for adsorption studies and on-line preconcentration of cobalt ions from aqueous medium. Chem. Eng. J. 239, 233–241.

Dobrowolski, R., Otto, M., 2012. Determination of nickel and cobalt in reference plant materials by carbon slurry sampling GFAAS technique after their simultaneous preconcentration onto modified activated carbon. J. Food Compos. Anal. 26, 58–65.

Du, Y., Chen, M., Zhang, Y., Luo, F., He, C., Li, M., Chen, X., 2013. Determination of iron(III) based on the fluorescence quenching of rhodamine B derivative. Talanta 106, 261–265.

El Haddad, M., Mamouni, R., Saffaj, N., Lazar, Said, 2012. Removal of a cationic dye – Basic Red 12 – from aqueous solution by

adsorption onto animal bone meal. J. Assoc. Arab Univ. Basic Appl. Sci. 12, 48–54.

El-ghamry, M.A., Saleh, A.A., Khalil, S.M.E., Mohammed, A.A., 2013. Mono, bi- and trinuclear metal complexes derived from new benzene-1,4-bis(3-pyridin-2-ylurea) ligand. Spectral, magnetic, thermal and 3D molecular modeling studies. Spectrochim. Acta Part A 110, 205–216.

El-Shahat, M.F., Moawed, E.A., Zaid, M.A.A., 2003. Preconcentration and separation of iron, zinc, cadmium and mercury, from waste water using Nile blue a grafted polyurethane foam. Talanta 59, 851–866.

Emara, A.A.A., Tawab, M.A., El-ghamry, M.A., Elsabee, M.Z., 2011. Metal uptake by chitosan derivatives and structure studies of the polymer metal complexes. Carbohydr. Polym. 83, 192–202.

Gómez-Nieto, B., Gismeran, M.J., Sevilla, M.T., Procopio, J.R., 2013. Simultaneous and direct determination of iron and nickel in biological solid samples by high-resolution continuum source graphite furnace atomic absorption spectrometry. Talanta 116, 860–865.

He, J., Chen, J.P., 2014. A comprehensive review on biosorption of heavy metals by algal biomass: materials, performances, chemistry, and modeling simulation tools. Bioresour. Technol. 160, 67–78.

Ismail, T.M.A., Saleh, A.A., El Ghamry, M.A., 2012. Tetra- and hexadentate Schiff base ligands and their Ni(II), Cu(II) and Zn(II) complexes. Synthesis, spectral, magnetic and thermal studies. Spectrochim. Acta Part A 86, 276–288.

Kassem, M.A., Amin, A.S., 2013. Spectrophotometric determination of iron in environmental and food samples using solid phase extraction. Food Chem. 141, 1941–1946.

Kumar, B.G.P., Shivakamy, K., Miranda, L.R., Velan, M., 2006. Preparation of steam activated carbon from rubber wood sawdust (Hevea brasiliensis) and its adsorption kinetics. J. Hazard. Mater. 136, 922–929.

Marczenko, Z., 1986. Spectrophotometric Determination of Elements, third ed. Ellis Horwood, Chichester.

Martins, A.F., Cardoso, A.L., Stahl, J.A., Diniz, J., 2007. Low temperature conversion of rice husks, eucalyptus sawdust and peach stones for the production of carbon like adsorbent. Bioresour. Technol. 98, 1095–1100.

Merli, D., Profumo, A., Dossi, C., 2012. An analytical method for Fe (II) and Fe(III) determination in pharmaceutical grade iron sucrose complex and sodium ferric gluconate complex. J. Pharm. Anal. 2, 450–453.

Moawed, E.A., 2013. Effect of heating processes on Salvadora persica (Miswak) and its application for removal and determination of aniline blue from wastewater. J. Taibah Univ. Sci. 7, 26–34.

Moawed, E.A., Abulkibash, A.B., 2012. Selective separation of Light green and Safranin O from aqueous solution using Salvadora persica (Miswak) powder as a new biosorbent. J. Saudi Chem. Soc., 1–8, http: //dxdoi.org/10.1016/ j.jscs. 2012.10.011.

Moawed, E.A., Burham, N., El-Shahat, M.F., 2013. Separation and determination of iron and manganese in water using polyhydroxyl polyurethane foam. J. Assoc. Arab Univ. Basic Appl. Sci. 14, 60–66.

Moawed, E.A., Ishaq, I., Abdul-Rahman, A., El-Shahat, M.F., 2014. Synthesis, characterization of carbon polyurethane powder and its application for separation and spectrophotometric determination of platinum in pharmaceutical and ore samples. Talanta 121, 113–121.

Nadeem, R., Zafar, M.N., Afzal, A., Hanif, M.A., Saeed, R., 2014. Potential of NaOH pretreated Mangifera indica waste biomass for the mitigation of Ni(II) and Co(II) from aqueous solutions. J. Taiwan Inst. Chem. Eng. 45, 967–972.

Naeini, A., Naderi, N.J., Shokr, H., 2014. Analysis and in vitro anti-Candida antifungal activity of Cuminum cyminumand Salvadora persica herbs extracts against pathogenic Candida strains. J. Med. Mycol. 24, 13–18.

Namasivayam, C., Sangeetha, D., 2005. Kinetic studies of adsorption of thiocyanate onto $ZnCl_2$ activated carbon from coir pith, an agricultural solid waste. Chemosphere 60, 1616–1623.

Namasivayam, C., Sangeetha, D., Gunasekaran, R., 2007. Removal of anions, heavy metals, organics and dyes from water by adsorption onto a new activated carbon from jatropha husk an agro-industrial solid waste. Trans. IChemE Part B: Process Saf. Environ. Prot. 85, 181–184.

Naushad, Mu., Khan, M.A., AL-Othman, Z.A, Khan, M.R., 2014. Adsorptive removal of nitrate from synthetic and commercially available bottled water samples using De-Acidite FF-IP resin. J. Ind. Eng. Chem. 20, 3400–3407.

Naushad, Mu., AL-Othman, Z.A., 2015. Separation of toxic Pb^{2+} metal from aqueous solution using strongly acidic cation-exchange resin: analytical applications for the removal of metal ions from pharmaceutical formulation. Desalin. Water Treat. 53, 2158–2166.

Naushad, Mu., Mittal, A., Rathore, M., Gupta, V., 2015a. Ion-exchange kinetic studies for Cd(II), Co(II), Cu(II), and Pb(II) metal ions over a composite cation exchanger. Desalin. Water Treat. 54, 2883–2890.

Naushad, Mu., AL-Othman, Z.A., Awual, Md.R., Alam, M.M., 2015b. Adsorption kinetics, isotherms, and thermodynamic studies for the adsorption of Pb^{2+} and Hg^{2+} metal ions from aqueous medium using Ti(IV) iodovanadate cation exchanger. Ionics 21, 2237–2245.

Oguz, E., Ersoy, M., 2014. Biosorption of cobalt(II) with sun flower biomass from aqueous solutions in a fixed bed column and neural networks modeling. Ecotoxicol. Environ. Saf. 99, 54–60.

Pourjavid, M.R., Sehat, A.A., Arabieh, M., Yousefi, S.R., Hosseini, M.H., Rezaee, M., 2014. Column solid phase extraction and flame atomic absorption spectrometric determination of manganese(II) and iron(III) ions in water, food and biological samples using 3-(1-methyl-1H-pyrrol-2-yl)-1H-pyrazole-5-carboxylic acid on synthesized graphene oxide. Mater. Sci. Eng. C 35, 370–378.

Rezaei, B., Ensafi, A.A., Shandiz, F., 2001. Simultaneous determination of cobalt and nickel by spectrophotometric method and artificial neural network. Microchem. J. 70, 35–40.

Shebl, M., El-ghamry, M.A., Khalil, S.M.E., Kishk, M.A.A., 2014. Mono- and binuclear copper(II) complexes of new hydrazone ligands derived from 4,6-diacetylresorcinol: synthesis, spectral studies and antimicrobial activity. Spectrochim. Acta Part A 126, 232–241.

Tuzen, M., Soylak, M., Elci, L., 2005. Multi-element pre-concentration of heavy metal ions by solid phase extraction on Chromosorb 108. Anal. Chim. Acta 548, 101–108.

Ververis, C., Georghiou, K., Danielidis, D., Hatzinikolaou, D.G., Santas, P., Santas, R., Corleti, V., 2007. Cellulose, hemicelluloses, lignin and ash content of some organic materials and their suitability for use as paper pulp supplements. Bioresour. Technol. 98, 296–301.

Wen, X., He, L., Shi, C., Deng, Q., Wang, J., Zhao, X., 2013. Application of rapid cloud point extraction method for trace cobalt analysis coupled with spectrophotometric determination. Spectrochim. Acta Part A 115, 452–456.

Xu, H., Zhang, W., Zhang, X., Wang, J., Wang, J., 2013. Simultaneous preconcentration of cobalt, nickel and copper in water samples by cloud point extraction method and their determination by flame atomic absorption spectrometry. Procedia Environ. Sci. 18, 258–263.

Zeng, C., Jia, Y., Lee, Y., Hou, X., Wu, L., 2012. Ultrasensitive determination of cobalt and nickel by atomic fluorescence spectrometry using APDC enhanced chemical vapor generation. Microchem. J. 104, 33–37.